# Supportive Information

## Multifunctional MRI/PET Nanobeacons Derived from the In situ Self-Assembly of Translational Polymers and Clinical Cargo through Coalescent Intermolecular Forces

Charalambos Kaittanis[1,2], Travis M. Shaffer[1,3], Alexander Bolaender[1], Zachary Appelbaum[1], Jeremy Appelbaum[1], Gabriela Chiosis[1], Jan Grimm[1, 4, 5, 6*]

[1]Molecular Pharmacology Program, [4]Department of Radiology, Memorial Sloan Kettering Cancer Center, 1275 York Avenue, New York, NY 10065, USA
[2] Center for Advanced Medical Imaging Sciences, Department of Radiology, Massachusetts General Hospital, 55 Fruit Street, Boston, MA 02114.
[3]Department of Chemistry, Hunter College and Graduate Center of the City University of New York, New York, NY 10065, USA
[5]Department of Pharmacology and [6]Radiology, Weill Cornell Medical College, New York, NY 10065, USA

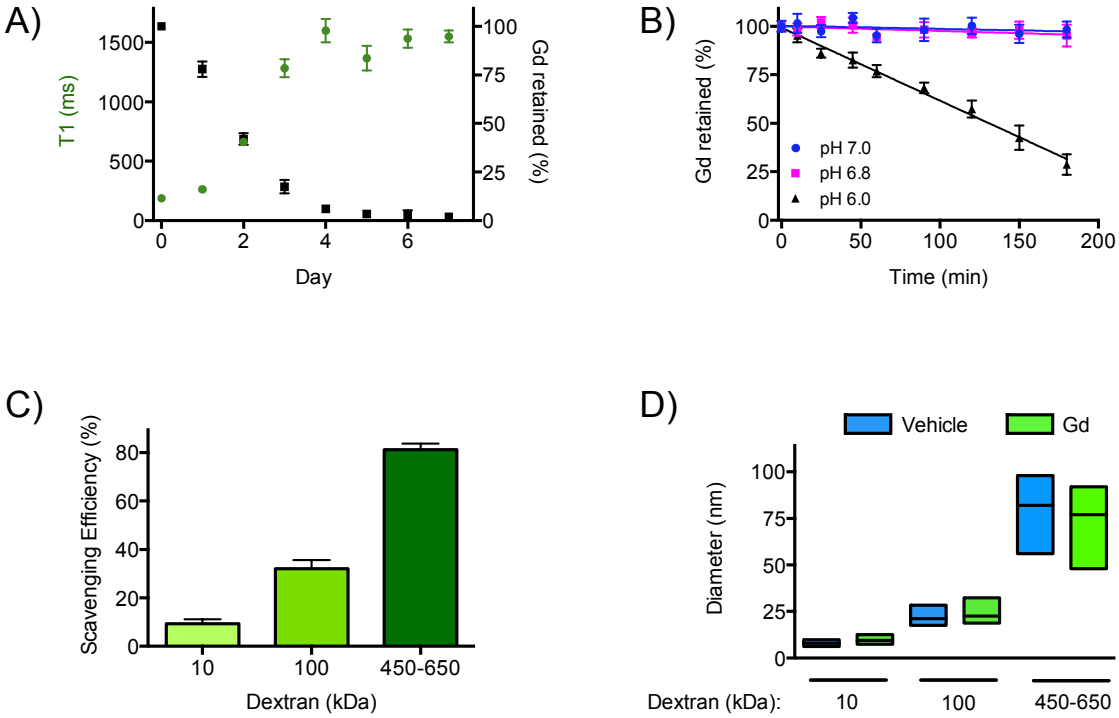

**Figure S1.** Retention of gadolinium (Gd) by carbohydrate PNPs. **A)** The PNPs that chelated Gd at room temperature slowly released the tracer in serum, indicated by increases in the PNP solution's T1 signal. **B)** When the Gd chelation at room temperature, the PNPs unloaded gadolinium once the pH reached 6.0. **C)** PNP of high-molecular-weight dextran chelated Gd more efficiently, **D)** whereas Gd chelation did not affect the nanoparticles size and distribution. Means ± SEM.

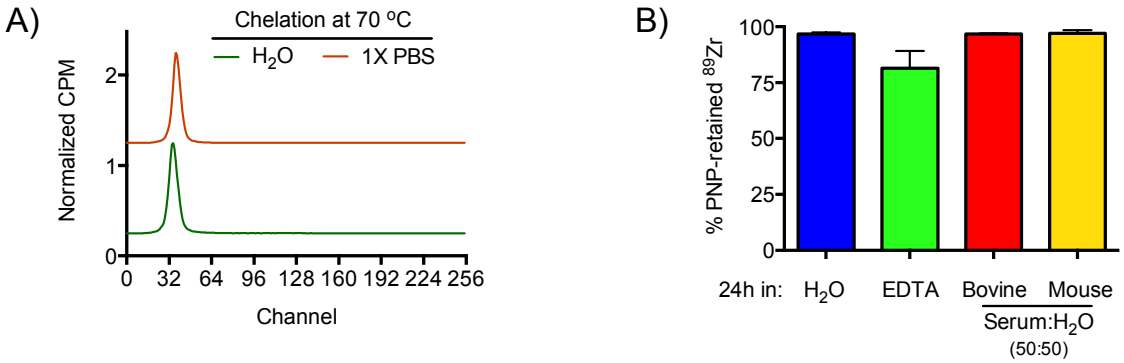


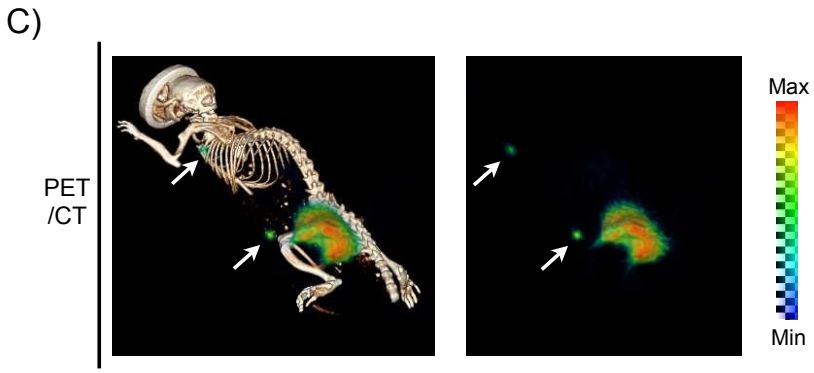


**Figure S2.** Chelation and imaging with $^{89}$Zr-PNPs. **A)** The PNPs effectively chelated $^{89}$Zr after 30-min heating at 70 °C, as shown by the radio-ITLC chromatograms. **B)** After chelation at 70 °C, the stability of the PNP – $^{89}$Zr association was evaluated, which showed that the PNPs retained the radiotracer under EDTA challenge, and in fetal bovine and mouse sera. Means ± SEM. **C)** CT/PET (left) and PET only (right) of draining lymph nodes (white arrows) after peritumoral administration of $^{89}$Zr-PNPs, revealing proximal and distal drainage through the afferent lymphatics.

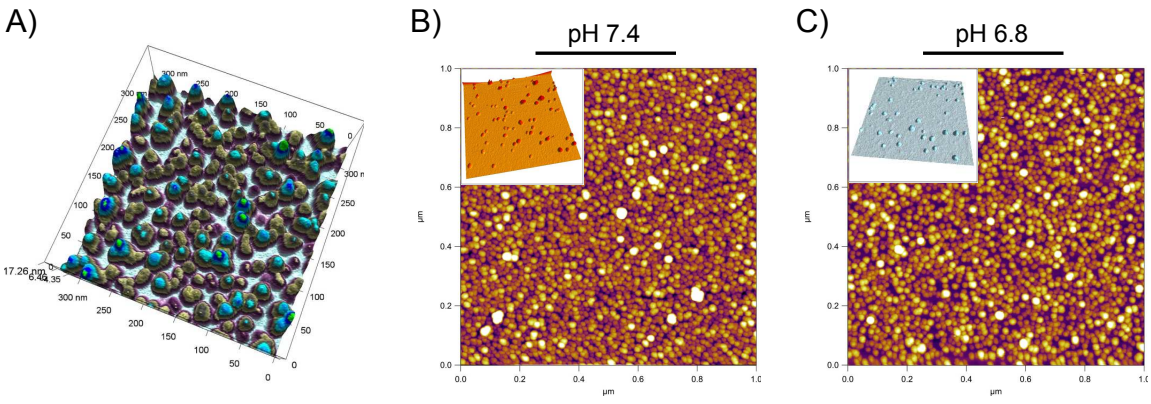


**Figure S3.** Atomic force microscopy performed at liquid state showed the structural stability of the PNPs after cargo loading and release. **A)** Distribution of the unloaded PNPs. Doxorubicin-loaded PNPs after incubation at **B)** pH 7.4 and **C)** pH 6.8. (**insets** show higher dilutions of the two samples, with the PNP being monodispersed).

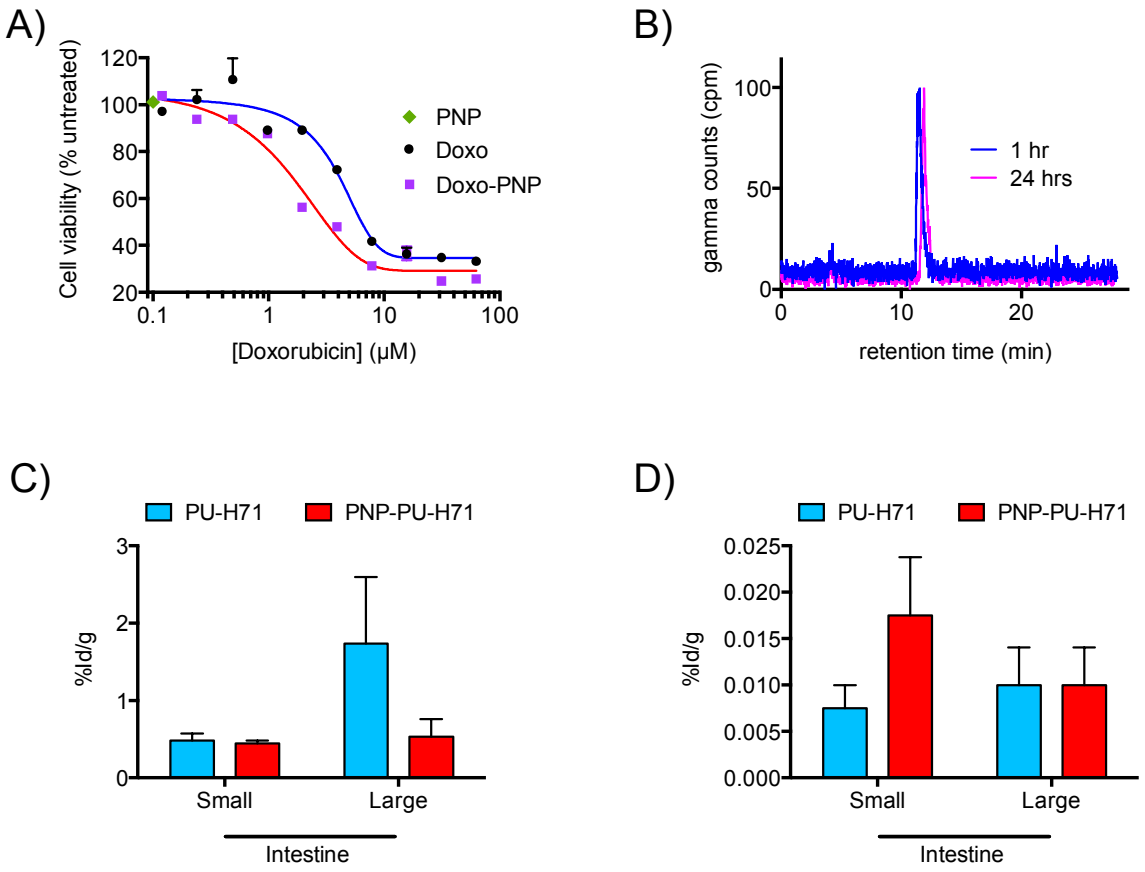


**Figure S4. A)** Doxorubicin-loaded dextran nanophores cause more cell death than free doxorubicin in the androgen-receptor-negative human prostate cancer cell line PC3. (PNP: unloaded nanoparticles; Doxo: Doxorubicin; Doxo-PNP: doxorubicin-loaded PNPs) The unloaded PNP are not toxic to the cells. **B)** Serum stability of $^{131}$I-PU-H71 determined through HPLC, after 1 and 24-hour incubation in mouse serum. Intestinal excretion of free and PNP-loaded $^{131}$I-PU-H71 **C)** 4 h and **D)** 24 h post i.v. administration (%ID/g: % injected dose/tissue mass). Means ± SEM.

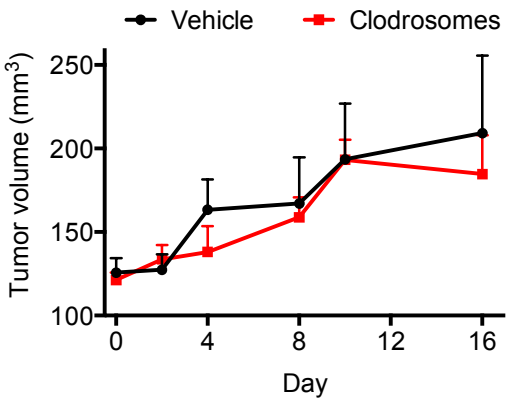


**Figure S5.** Tumor growth response after clodrosome-based therapy of athymic, male nude mice with LNCaP xenografts on their flanks ($n_{vehicle}$=$n_{Clodrosomes}$ =5). Means ± SEM.

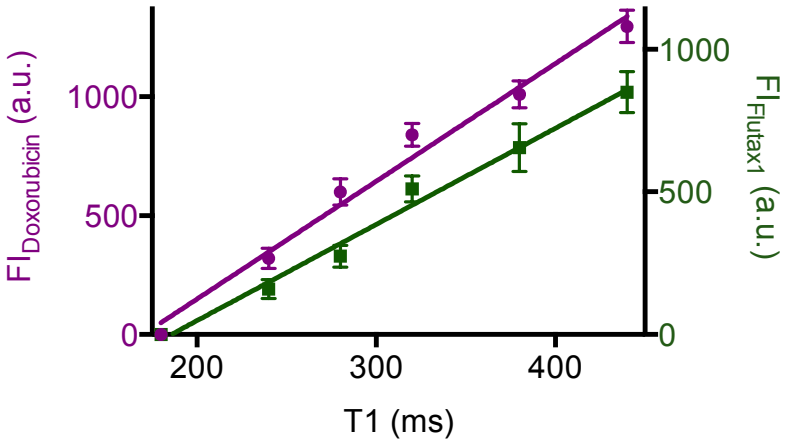


**Figure S6.** The loading of molecular cargos into PNP affects the nanoparticles' magnetic resonance signal. Gd-retaining PNP were co-loaded with Doxorubicin ($\lambda_{ex}$ = 485 nm, $\lambda_{em}$ = 590 nm) and Flutax1 ($\lambda_{ex}$ = 495 nm, $\lambda_{em}$ = 520 nm), which caused increased in the T1 relaxation times. Means ± SEM.